

Special Issue: Bio-based Packaging

Guest Editors: José M. Lagarón, Amparo López-Rubio, and María José Fabra
Institute of Agrochemistry and Food Technology of the Spanish Council for Scientific Research

EDITORIAL

Bio-based Packaging

J. M. Lagarón, A. López-Rubio and M. J. Fabra, *J. Appl. Polym. Sci.* 2015,
DOI: 10.1002/app.42971

REVIEWS

Active edible films: Current state and future trends

C. Mellinas, A. Valdés, M. Ramos, N. Burgos, M. D. C. Garrigós and A. Jiménez,
J. Appl. Polym. Sci. 2015, DOI: 10.1002/app.42631

Vegetal fiber-based biocomposites: Which stakes for food packaging applications?

M.-A. Berthet, H. Angellier-Coussy, V. Guillard and N. Gontard, *J. Appl. Polym. Sci.* 2015, DOI: 10.1002/app.42528

Enzymatic-assisted extraction and modification of lignocellulosic plant polysaccharides for packaging applications

A. Martínez-Abad, A. C. Ruthes and F. Vilaplana, *J. Appl. Polym. Sci.* 2015, DOI: 10.1002/app.42523

RESEARCH ARTICLES

Combining polyhydroxyalkanoates with nanokeratin to develop novel biopackaging structures

M. J. Fabra, P. Pardo, M. Martínez-Sanz, A. Lopez-Rubio and J. M. Lagarón, *J. Appl. Polym. Sci.* 2015, DOI: 10.1002/app.42695

Production of bacterial nanobiocomposites of polyhydroxyalkanoates derived from waste and bacterial nanocellulose by the electrospinning enabling melt compounding method

M. Martínez-Sanz, A. Lopez-Rubio, M. Villano, C. S. S. Oliveira, M. Majone, M. Reis and J. M. Lagarón, *J. Appl. Polym. Sci.* 2015,
DOI: 10.1002/app.42486

Bio-based multilayer barrier films by extrusion, dispersion coating and atomic layer deposition

J. Vartiainen, Y. Shen, T. Kaljunen, T. Malm, M. Vähä-Nissi, M. Putkonen and A. Harlin, *J. Appl. Polym. Sci.* 2015,
DOI: 10.1002/app.42260

Film blowing of PHBV blends and PHBV-based multilayers for the production of biodegradable packages

M. Cunha, B. Fernandes, J. A. Covas, A. A. Vicente and L. Hilliou, *J. Appl. Polym. Sci.* 2015, DOI: 10.1002/app.42165

On the use of tris(nonylphenyl) phosphite as a chain extender in melt-blended poly(hydroxybutyrate-co-hydroxyvalerate)/clay nanocomposites: Morphology, thermal stability, and mechanical properties

J. González-Ausejo, E. Sánchez-Safont, J. Gámez-Pérez and L. Cabedo, *J. Appl. Polym. Sci.* 2015, DOI: 10.1002/app.42390

Characterization of polyhydroxyalkanoate blends incorporating unpurified biosustainably produced poly(3-hydroxybutyrate-co-3-hydroxyvalerate)

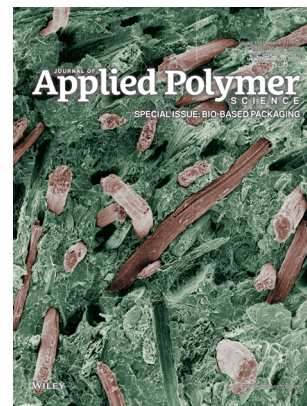
A. Martínez-Abad, L. Cabedo, C. S. S. Oliveira, L. Hilliou, M. Reis and J. M. Lagarón, *J. Appl. Polym. Sci.* 2015,
DOI: 10.1002/app.42633

Modification of poly(3-hydroxybutyrate-co-3-hydroxyvalerate) properties by reactive blending with a monoterpene derivative

L. Pilon and C. Kelly, *J. Appl. Polym. Sci.* 2015, DOI: 10.1002/app.42588

Poly(3-hydroxybutyrate-co-3-hydroxyvalerate) films for food packaging: Physical-chemical and structural stability under food contact conditions

V. Chea, H. Angellier-Coussy, S. Peyron, D. Kemmer and N. Gontard, *J. Appl. Polym. Sci.* 2015, DOI: 10.1002/app.41850



Special Issue: Bio-based Packaging

Guest Editors: José M. Lagarón, Amparo López-Rubio, and María José Fabra
Institute of Agrochemistry and Food Technology of the Spanish Council for Scientific Research

Impact of fermentation residues on the thermal, structural, and rheological properties of polyhydroxy(butyrate-co-valerate) produced from cheese whey and olive oil mill wastewater
L. Hilliou, D. Machado, C. S. S. Oliveira, A. R. Gouveia, M. A. M. Reis, S. Campanari, M. Villano and M. Majone, *J. Appl. Polym. Sci.* 2015, DOI: [10.1002/app.42818](https://doi.org/10.1002/app.42818)

Synergistic effect of lactic acid oligomers and laminar graphene sheets on the barrier properties of polylactide nanocomposites obtained by the in situ polymerization pre-incorporation method
J. Ambrosio-Martín, A. López-Rubio, M. J. Fabra, M. A. López-Manchado, A. Sorrentino, G. Gorrasi and J. M. Lagarón, *J. Appl. Polym. Sci.* 2015, DOI: [10.1002/app.42661](https://doi.org/10.1002/app.42661)

Antibacterial poly(lactic acid) (PLA) films grafted with electrospun PLA/allyl isothiocyanate fibers for food packaging
H. H. Kara, F. Xiao, M. Sarker, T. Z. Jin, A. M. M. Sousa, C.-K. Liu, P. M. Tomasula and L. Liu, *J. Appl. Polym. Sci.* 2015, DOI: [10.1002/app.42475](https://doi.org/10.1002/app.42475)

Poly(L-lactide)/ZnO nanocomposites as efficient UV-shielding coatings for packaging applications
E. Lizundia, L. Ruiz-Rubio, J. L. Vilas and L. M. León, *J. Appl. Polym. Sci.* 2015, DOI: [10.1002/app.42426](https://doi.org/10.1002/app.42426)

Effect of electron beam irradiation on the properties of polylactic acid/montmorillonite nanocomposites for food packaging applications
M. Salvatore, A. Marra, D. Duraccio, S. Shayanfar, S. D. Pillai, S. Cimmino and C. Silvestre, *J. Appl. Polym. Sci.* 2015, DOI: [10.1002/app.42219](https://doi.org/10.1002/app.42219)

Preparation and characterization of linear and star-shaped poly L-lactide blends
M. B. Khajeheian and A. Rosling, *J. Appl. Polym. Sci.* 2015, DOI: [10.1002/app.42231](https://doi.org/10.1002/app.42231)

Mechanical properties of biodegradable polylactide/poly(ether-block-amide)/thermoplastic starch blends: Effect of the crosslinking of starch
L. Zhou, G. Zhao and W. Jiang, *J. Appl. Polym. Sci.* 2015, DOI: [10.1002/app.42297](https://doi.org/10.1002/app.42297)

Interaction and quantification of thymol in active PLA-based materials containing natural fibers
I. S. M. A. Tawakkal, M. J. Cran and S. W. Bigger, *J. Appl. Polym. Sci.* 2015, DOI: [10.1002/app.42160](https://doi.org/10.1002/app.42160)

Graphene-modified poly(lactic acid) for packaging: Material formulation, processing, and performance
M. Barletta, M. Puopolo, V. Tagliaferri and S. Vesco, *J. Appl. Polym. Sci.* 2015, DOI: [10.1002/app.42252](https://doi.org/10.1002/app.42252)

Edible films based on chia flour: Development and characterization
M. Dick, C. H. Pagno, T. M. H. Costa, A. Gomaa, M. Subirade, A. De O. Rios and S. H. Flóres, *J. Appl. Polym. Sci.* 2015, DOI: [10.1002/app.42455](https://doi.org/10.1002/app.42455)

Influence of citric acid on the properties and stability of starch-polycaprolactone based films
R. Ortega-Toro, S. Collazo-Bigliardi, P. Talens and A. Chiralt, *J. Appl. Polym. Sci.* 2015, DOI: [10.1002/app.42220](https://doi.org/10.1002/app.42220)

Bionanocomposites based on polysaccharides and fibrous clays for packaging applications
A. C. S. Alcântara, M. Darder, P. Aranda, A. Ayral and E. Ruiz-Hitzky, *J. Appl. Polym. Sci.* 2015, DOI: [10.1002/app.42362](https://doi.org/10.1002/app.42362)

Hybrid carrageenan-based formulations for edible film preparation: Benchmarking with kappa carrageenan
F. D. S. Larotonda, M. D. Torres, M. P. Gonçalves, A. M. Sereno and L. Hilliou, *J. Appl. Polym. Sci.* 2015, DOI: [10.1002/app.42263](https://doi.org/10.1002/app.42263)



Special Issue: Bio-based Packaging

Guest Editors: José M. Lagarón, Amparo López-Rubio, and María José Fabra
Institute of Agrochemistry and Food Technology of the Spanish Council for Scientific Research

Structural and mechanical properties of clay nanocomposite foams based on cellulose for the food packaging industry

S. Ahmadzadeh, J. Keramat, A. Nasirpour, N. Hamdami, T. Behzad, L. Aranda, M. Vilasi and S. Desobry, *J. Appl. Polym. Sci.* 2015, DOI: [10.1002/app.42079](https://doi.org/10.1002/app.42079)

Mechanically strong nanocomposite films based on highly filled carboxymethyl cellulose with graphene oxide

M. El Achaby, N. El Miri, A. Snik, M. Zahouily, K. Abdelouahdi, A. Fihri, A. Barakat and A. Solhy, *J. Appl. Polym. Sci.* 2015, DOI: [10.1002/app.42356](https://doi.org/10.1002/app.42356)

Production and characterization of microfibrillated cellulose-reinforced thermoplastic starch composites

L. Lendvai, J. Karger-Kocsis, Á. Kmetty and S. X. Drakopoulos, *J. Appl. Polym. Sci.* 2015, DOI: [10.1002/app.42397](https://doi.org/10.1002/app.42397)

Development of bioplastics based on agricultural side-stream products: Film extrusion of *Crambe abyssinica*/wheat gluten blends for packaging purposes

H. Rasel, T. Johansson, M. Gällstedt, W. Newson, E. Johansson and M. Hedenqvist, *J. Appl. Polym. Sci.* 2015, DOI: [10.1002/app.42442](https://doi.org/10.1002/app.42442)

Influence of plasticizers on the mechanical and barrier properties of cast biopolymer films

V. Jost and C. Stramm, *J. Appl. Polym. Sci.* 2015, DOI: [10.1002/app.42513](https://doi.org/10.1002/app.42513)

The effect of oxidized ferulic acid on physicochemical properties of bitter vetch (*Vicia ervilia*) protein-based films

A. Arabestani, M. Kadivar, M. Shahedi, S. A. H. Goli and R. Porta, *J. Appl. Polym. Sci.* 2015, DOI: [10.1002/app.42894](https://doi.org/10.1002/app.42894)

Effect of hydrochloric acid on the properties of biodegradable packaging materials of carboxymethylcellulose/poly(vinyl alcohol) blends

M. D. H. Rashid, M. D. S. Rahaman, S. E. Kabir and M. A. Khan, *J. Appl. Polym. Sci.* 2015, DOI: [10.1002/app.42870](https://doi.org/10.1002/app.42870)



Production and characterization of microfibrillated cellulose-reinforced thermoplastic starch composites

László Lendvai,¹ József Karger-Kocsis,^{1,2} Ákos Kmetty,^{1,2} Stavros X. Drakopoulos^{1,3}

¹Department of Polymer Engineering, Faculty of Mechanical Engineering, Budapest University of Technology and Economics, Muegyetem rkp. 3., H-1111 Budapest, Hungary

²MTA-BME Research Group for Composite Science and Technology, Muegyetem rkp. 3., H-1111 Budapest, Hungary

³Department of Materials Science, University of Patras, Patras, GR-26504, Greece

Correspondence to: J. Karger-Kocsis (E-mail: karger@pt.bme.hu)

ABSTRACT: In this study thermoplastic starch (TPS) matrix-based microfibrillated cellulose (MFC) reinforced microcomposites were prepared via extrusion compounding in one-step. Starch was plasticized with a combination of glycerol and water. The native starch/glycerol and the plasticized starch/water ratios were set for 4/1 and 6/1, respectively. Two different MFC types (of varying mean length and diameter) were incorporated up to 20 wt % in the plasticizer-containing premix prior to its compounding in a twin-screw extruder. The mechanical properties of the TPS biocomposites were markedly enhanced by the introduction of MFC. The yield strength was improved by ~50%, whereas the stiffness by ~250% upon adding 20 wt % MFC compared to the parent TPS. Dynamic mechanical analysis (DMA) revealed that the reinforcing effect of the MFC was more prominent in the starch- than in the glycerol (plasticizer)-rich phase of the TPS. The mean length and diameter of the MFCs, yielding similar aspect ratio values lying below the estimated critical one, influenced the mechanical, thermal, and thermo-mechanical properties marginally. © 2015 Wiley Periodicals, Inc. *J. Appl. Polym. Sci.* **2016**, *133*, 42397.

KEYWORDS: biomaterials; cellulose and other wood products; extrusion; morphology; packaging

Received 8 January 2015; accepted 21 April 2015

DOI: 10.1002/app.42397

INTRODUCTION

There is a growing interest nowadays in reducing the amount of waste which is caused by the disposable packaging mainly from petroleum-based plastics. Therefore, a large body of works has been already devoted to develop polymers from renewable resources. The related studies often addressed the development of fully bio-based and thus biodegradable packaging materials. Thermoplastic starch (TPS) is considered as one of the most promising biomaterials for packaging purpose, mainly because of its low price and biodegradability.^{1–6} Note that starch is a renewable feedstock considering the fact that it can be recovered from numerous plants (potato, corn, sago, etc.).⁵ TPS may serve as a “green” packaging material, which can be produced using common thermoplastic processing technologies thereby considering some specific characteristics of starch.¹ Starch itself is a polysaccharide having no thermoplastic feature; however, it can be brought into a “thermoplastic-like” state under specific conditions (using plasticizer and/or mechanical shear).^{7,8} Melt compounding of thermoplastic materials is performed mostly in an internal mixer or in single- or twin-screw extruders. While internal mixing is a batch-type method, extrusion is a continu-

ous process, which is not only a cost-efficient route but also allows for the combination of thermoplastic polymers with other polymers and/or reinforcements.^{2,5,9,10} By using one- or two-step extrusion process the properties (mechanical, thermal, barrier...) of the TPS-based systems can be tuned to meet the application requirements. For TPS material development, however, other techniques such as dissolution followed by solution casting can also be used.^{3,5,11–13}

Like any common thermoplastic polymer, starch can be processed via melt compounding techniques in presence of suitable plasticizers.^{2,9,14} Various plasticizers have been tried to convert starch into TPS but the most widely used ones are water, polyols (e.g., glycerol), vegetable oils, and sorbitol.^{9,15–17} Being a by-product of biodiesel production glycerol is low priced and thus especially suited for mass production of TPS even if the mechanical properties of sorbitol plasticized TPS have been found to be slightly better.¹⁶ The amount of plasticizer used can be varied in certain limits to adjust the stiffness and strength of TPS to our needs. However, one has to bear in mind that if the plasticizer content in the mixture is not optimal, processing issues are often encountered,^{4,18} also leading to the presence of

residual granules (referred to “ghost granules” in the literature.^{1,4}). The presence of these ghost granules decreases the mechanical properties and gives a hazy appearance of the originally transparent material. This should be avoided in many cases, especially for selected packaging applications.

Among the main disadvantages of TPS its hydrophilic character and poor mechanical properties should be mentioned. From this reason many studies have addressed the improvement of the properties of TPS.^{3,9,10,12,17,19} Trials, done so far, include chemical modifications, grafting, blending with other biopolymers, and also the incorporation of a reinforcing particles.^{3,5,9,11–13,17,20–24} Main goal of these studies was to improve the properties, while still preserving the biodegradability of the related TPS-based systems. As far as particulate fillers and reinforcements is concerned, the most promising ones for TPS are cellulose and layered silicates. These additives can improve the mechanical and barrier properties which are of great relevance for packaging. The dispersion of these particles and its effect on the properties of TPS were already topics of some publications.^{5,9,10,13,15,17,19,25} Extensive kneading associated with melt shearing during extrusion support the disintegration of the entangled cellulose micro- and nanofibers when introduced in dry form. Extrusion melt compounding is also the right way when these cellulosic fillers are incorporated from a premix or aqueous dispersion.^{9,26} In the latter case vent ports of the extruder may work for the evaporation of the excess water as discussed later.

Cellulose of natural origin may serve in both micro- and nanofiber forms as reinforcements for polymers.²⁷ There is a growing interest of using micro- and nanocellulose as property modifiers for different kind of polymers,^{28,29} including TPS. The main advantage in using of cellulosic fibers into TPS-based composites is that their biodegradability and bio-based features are maintained. This is the major driving force for ongoing studies in this field.^{9,17,19,30,31}

When fabricating polymer composites with micro- and nanoscale particles, the main problem is to achieve the homogenous and fine dispersion of the particles within the polymer matrix³² as these particulates tend to form agglomerates, bundles. As a consequence the large particles' agglomerates may act as stress concentration sites causing premature failure of the materials and in case of fibrous bundles the high aspect ratio of the constituent fibrils cannot be exploited for reinforcing effect. Thus the quality of the dispersion of the particles influences the properties of the corresponding composites significantly.³³ There are numerous methods to support the proper dispersion of micro- and nanosized particles in thermoplastics, such as *in situ* polymerization, solvent-assisted techniques, and traditional melt mixing. In the latter case the agglomerates and bundles are disrupted under action of the shear stresses developed. A relative new way is to introduce the particles in their aqueous dispersion or slurry during melt compounding of suitable thermoplastics.³⁴ Note that in this approach water works as a temporary carrier of the particles because it is removed downstream during the extrusion. This technique improves the dispersion of particles, but may not be used universally owing to the hygrother-

mal decomposition of some polymers. There are some cases however, when water works as a plasticizer for the given materials and thus should not be totally removed during melt mixing. An example for that is the production of TPS from natural starch.³⁴

This study was aimed at improving the properties of glycerol plasticized TPS by incorporating microfibrillated cellulose fibers (MFC) of different sizes (e.g., mean length and diameter) at various fiber content. The MFC-modified TPS was produced in a one-step melt extrusion compounding using a twin screw extruder. Morphology and structure of the prepared composites were characterized by scanning electron microscopy (SEM) and optical microscopy (OM). Specimens from MFC-modified TPS were subjected to static tensile tests and dynamic mechanical analysis (DMA) to check in what extent the MFC enhances the mechanical properties of TPS. The thermal degradation behavior of the samples was examined through thermogravimetric analysis (TGA).

EXPERIMENTAL

Materials

Native corn starch (CS) Hungramid F Meritena 100 (obtained from Brenntag Ltd., Budapest, Hungary) was selected as matrix material. As plasticizers different amounts of glycerol (purity of 99.5%; purchased from Csepp Bt., Budapest, Hungary) and distilled water were used. Two types of microfibrillated cellulose (MFC): Arbocel[®] B 600 (average length of 60 μm , diameter of 20 μm) and the ultrafine Arbocel[®] UFC-100 (average length of 8 μm , diameter of 2 μm) were introduced as reinforcements (JRS GmbH, Rosenberg, Germany). The above mentioned mean values of the particles were provided by the producer. These data have been proved via SEM images taken from the two MFC types as shown in Figure 1. Note that the mean aspect ratio values of these MFCs are practically identical (~ 3 and ~ 4 for B 600 and UFC-100, respectively). Stearic acid (purchased from a local supplier ICC-Chemol Ltd., Budapest, Hungary) was used as lubricant for the TPS.

Processing of the Materials

The CS powder and the MFC were conditioned in a Memmert HCP153 (Frankfurt, Germany) humidification chamber at 30°C and a relative humidity (RH) of 50% for at least 168 h (h) prior to processing. This was done to ensure that the components have the same moisture content during the preparation of each mixture. The MFC was incorporated in a premix, composed of starch, plasticizer, and lubricant, through manual mixing before the melt compounding step.

Preparation of Premix. Firstly the components were weighed and premixed manually to achieve a “dry” mixture. The ratio of CS/glycerol was fixed to exactly 4:1 in every mixtures. The MFC content, introduced in this dry mix, was varied in a range from 0 to 20 wt %. Table I shows the recipes of the samples. Totally, 1500 g was prepared of each mixture. Furthermore 250 g water was added to a batch of 1500 g containing all components. It is not listed in Table I. According to Tábi *et al.*⁴ 1 wt % stearic acid (with respect to whole amount) was added as well to

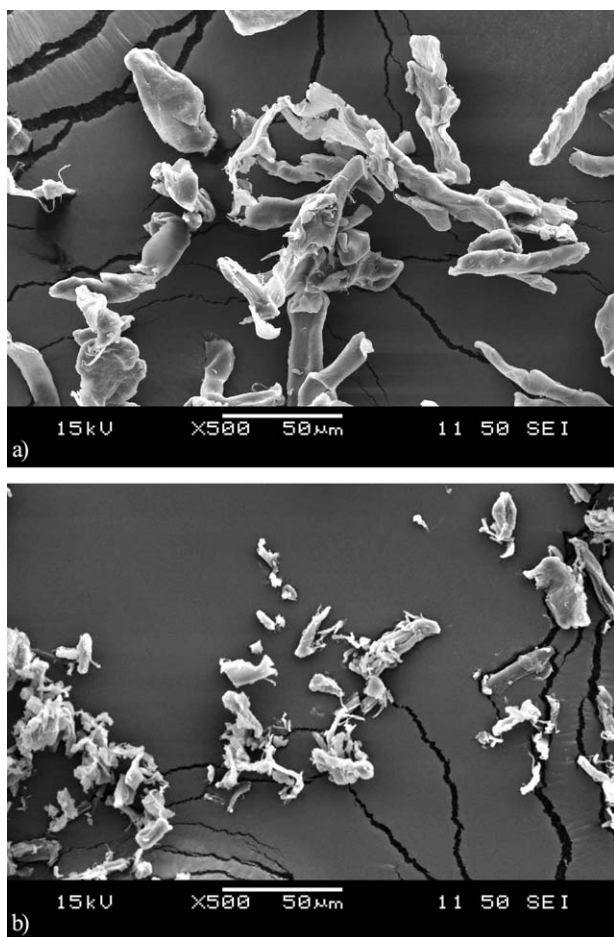


Figure 1. SEM images taken from raw MFC particles B 600 (a) and UFC-100 (b).

prevent the material sticking to the screws or to the die during the extrusion.

Compounding Process. As second step the dry mixtures were melt-compounded using a twin-screw extruder (LTE 26–44, Labtech Engineering, Samutprakarn, Thailand) with an L/D ratio of 44 and a screw diameter of 26 mm. The screw speed was 75 revolutions per minute (rpm), and the temperature profile of the extruder zones is shown in Table II. The temperature

Table I. Recipes of the Premixes Used for the Preparation of TPS and TPS/MFC Microcomposites

Sample	Starch (wt %)	Glycerol (wt %)	MFC (wt %)	Type of MFC
TPS	80	20	–	–
TPS_B600_5	76	19	5	B 600
TPS_B600_10	72	18	10	B 600
TPS_B600_15	68	17	15	B 600
TPS_B600_20	64	16	20	B 600
TPS_UFC_10	72	18	10	UFC-100

Note the water amount, viz. 250 g water/1500 g material, and the stearic acid lubricant (1 wt %) are not listed in this table.

Table II. Temperature Zones of the Extruder

Zone Nr.	Temperature (°C)	Zone Nr.	Temperature (°C)
1	85	6	100
2	90	7	110
3	95	8	110
4	100	9	120
5	100	10	120

of the die was 120°C. Starve feeding of the extruder was done manually. The extruder barrel was equipped with an atmospheric vent (at heating zone 7 out of 10) to remove the vaporized water from the melt. Because of the remaining water content, the extrudate was still sticky when leaving through the die. Thus the extruded pellet was conditioned (30°C, 50% RH) for a week before further processing.

Compression Molding. After conditioning the granulated extrudates were compression molded to sheets of 1.7 mm thickness using a hot press machine (Teach-Line Platen Press 200E, Dr. Coltin GmbH, Munich, Germany) at the temperature of 130°C. Specimens for testing were punched of the compression molded sheets.

Characterization

Every single sample was conditioned under the same circumstances (30°C, 50% RH) for at least 168 h prior to the following tests to obtain reproducible results.

Static Tensile Tests. The static mechanical properties were determined by tensile tests performed on a universal testing machine (Zwick Z020, Ulm, Germany) at a cross head speed of 5 mm/min. Specimens (type: 3 according to EN ISO 8256) for tensile tests were previously conditioned as mentioned above. The tests were performed at room temperature (RT). The average value was derived from five parallel measurements.

Scanning Electron Microscopy (SEM). The fracture surfaces of the TPS/MFC composites were inspected in a scanning electron microscope (SEM; JEOL JSM 6380LA, Tokyo, Japan). Prior to their inspection, the samples were sputter-coated with gold/palladium alloy.

Optical Microscopy (OM). The polished surfaces of TPS and TPS/MFC microcomposites were inspected in an optical microscope (OM, Olympus BX51M, Hamburg, Germany) equipped with a camera CAMEDIA C-5060.

Dynamic Mechanical Analysis (DMA). A dynamic mechanical analyzer (DMA Q800, TA Instruments, New Castle, NJ) was used to assess the thermo-mechanical behavior of the samples. Tests were run in tension mode at a frequency of 1 Hz in the temperature range between –100 and 120°C at a heating rate of 3°C min⁻¹. Prior to the tests the surface of the specimens (thickness: 1.6 mm; width: 3.8 mm, clamped length: 10 mm) was coated with a silicon-based grease to avoid their drying during the test.³⁵

Thermogravimetric Analysis (TGA). A TGA Q500 thermogravimetric analyzer (TA Instruments, New Castle, NJ) was used to examine the thermal behavior of the samples. Tests were

Table III. Tensile Properties of Neat TPS and Related MFC Filled TPS Biocomposites

Sample code	Yield strength (MPa)	Young's modulus (GPa)	Elongation at yield point (%)	Elongation at break (%)
TPS	7.9 ± 0.6	0.30 ± 0.04	29.2 ± 4.9	31.9 ± 5.3
TPS_B600_5	9.1 ± 0.3	0.51 ± 0.03	6.5 ± 0.5	7.5 ± 0.4
TPS_B600_10	9.7 ± 0.4	0.56 ± 0.04	8.9 ± 0.9	9.8 ± 0.9
TPS_B600_15	9.8 ± 0.4	0.58 ± 0.05	7.3 ± 1.1	9.8 ± 0.4
TPS_B600_20	11.9 ± 1.4	0.72 ± 0.05	3.8 ± 0.8	3.9 ± 0.7
TPS_UFC_10	9.1 ± 0.9	0.52 ± 0.06	9.9 ± 2.0	11.0 ± 2.1

performed from RT to 600°C at a heating rate of 10°C min⁻¹ under nitrogen flow using a flowing rate of 50 mL min⁻¹.

RESULTS AND DISCUSSION

Tensile Mechanical Properties

The mechanical properties of the neat TPS and TPS/MFC microcomposites are summarized in Table III. Tensile properties, such as yield strength, elongation, and Young's modulus were evaluated from the stress-strain curves obtained from the prepared microcomposite specimens. The data in Table III indicates that incorporation of MFC enhanced both the yield strength and the Young's modulus. This fact refers to the reinforcing action while the low scatter in the data (mostly under 10%) implies to a proper dispersion of MFC particles in the TPS matrix. The yield strength increases from 7.9 to 11.9 MPa with increasing filler content from 0 to 20 wt %. It can be seen that with increasing filler content from 0 to 5 wt %, the strength increases by 1.2 MPa, while further filler loading (10 wt %, 15 wt %) only improves the yield strength of the parent TPS by 1.8 and 1.9 MPa, respectively. The same trend can be observed for the stiffness, as well. Possible explanation for this finding may be of morphological origin: MFC reinforces the plasticized phase of the TPS at its low contents (5–15 wt %). Further discussion on this topic will be provided in the DMA section. Nevertheless, considering the yield strength and Young's modulus there was a significant improvement for all microcomposites except TPS_B600_15. The rise of Young's modulus with increasing MFC content was even more remarkable. The value 0.72 GPa, measured for TPS_B600_20, is almost 250% of the parent TPS. The elongation at break, however, dropped from ~30 to ~4%. Interestingly, no such change was observed by Hietala *et al.*²⁶ when the TPS was modified by 10 wt % treated and untreated wood fiber and cellulose nanofiber. The related TPS was, however, differently and in lesser extent plasticized than in this study. Accordingly, TPS of the cited authors exhibited markedly higher tensile strength (24.2 MPa) and Young's modulus (1.36 GPa) than our TPS version (*cf.* Table III).

These results are in good accordance with other studies on the same field.^{9,30} Cao *et al.*³⁰ explain these changes in the mechanical properties as the effect of strong hydrogen bonding interactions between the TPS matrix and the cellulose. It is the right place to mention that fibrous reinforcements, when adhering well to the matrix, in thermoplastics generally reduce the ductility of the corresponding composites. Results in Table III also show that there is no significant difference between the effects

of the different MFC types. Typical stress-strain curves of TPS and TPS/MFC biocomposites are shown in Figure 2. Figure 2 clearly demonstrates that with increasing MFC contents both the stiffness (initial slope of the stress-strain curves) and strength are improved but the ductility (strain values) highly reduced. Comparing the stress-strain curves (and the related results in Table III) of the TPS with the different MFC types at 10 wt % loading one can notice that B 600 performed slightly better than UFC-100, though the aspect ratio of the latter is a bit higher. This can be reasoned by supposing that the inherent mean flaw size of the TPS is commensurable with that of the UFC-100. If it is so, then a proper dispersion of UFC-100 should yield higher ductility values than B 600 at the same content, which was found, in fact. The ductility increment is owing to an efficient stress redistribution between the inherent voids and small UFC-100 particles because none of them act as stress concentrator. By contrast, the large B 600 particles work as stress concentration sites causing ductility reduction.

With respect of the tensile properties it is straightforward to give an estimate on the critical fiber length (l_c) of MFC. Recall that the MFC types used differed markedly in their length and diameter data but not in the corresponding aspect ratios. l_c can be computed by:

$$l_c = \frac{\sigma_f d}{2\tau}, \quad (1)$$

where σ_f is the strength of the fiber, d is the diameter of the fiber, and τ is the interfacial shear strength between the matrix polymer and the reinforcing fiber. τ can be estimated in the

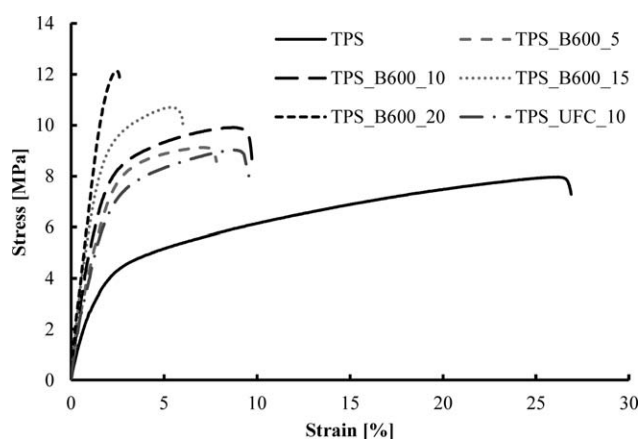


Figure 2. Typical stress-strain curves of TPS and TPS/MFC biocomposites.

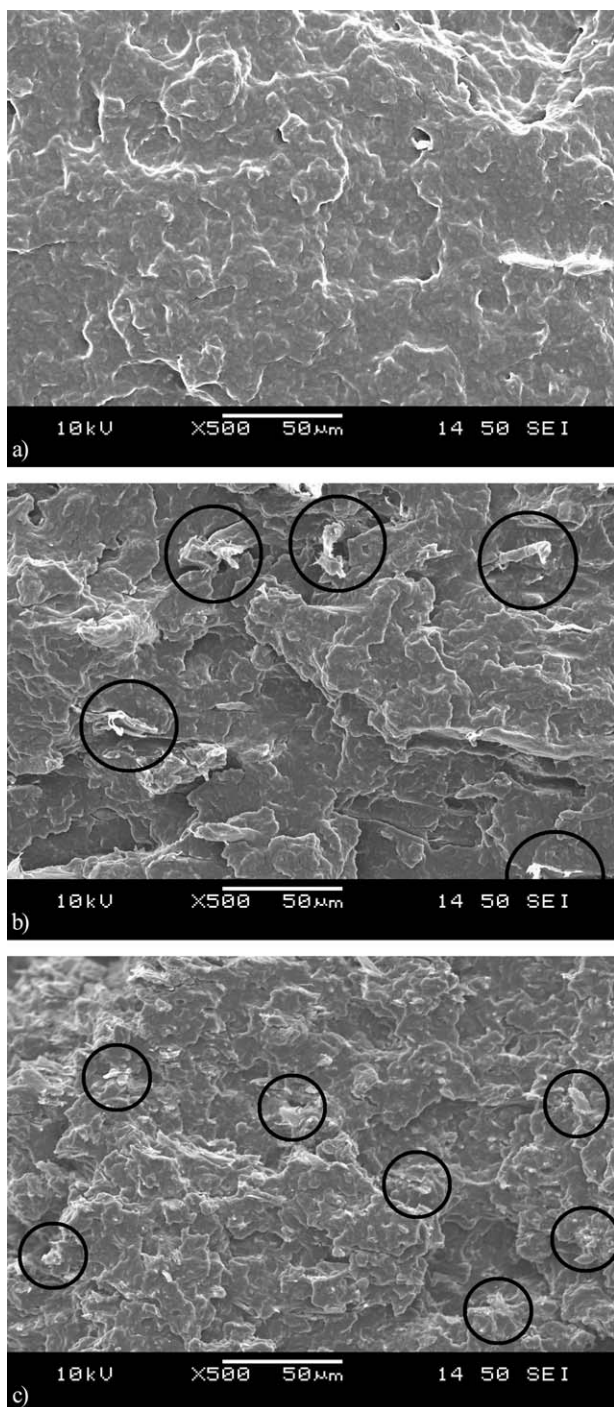


Figure 3. SEM pictures taken from the fracture surface of TPS (a) and TPS/MFC microcomposites (b,c). Designations: (a) TPS, (b) TPS_B600_10, (c) TPS_UFC_10.

knowledge of the matrix tensile strength (σ_m). For this purpose the same calculation has been used that was reported by Oksman *et al.*³⁶

$$\tau = \frac{\sigma_m}{\sqrt{3}}, \quad (2)$$

Considering the fact that $\sigma_m = 7.9$ MPa and accepting for $\sigma_f = 2000$ MPa³⁶ we can estimate the l_c values of MFCs B 600

and UFC-100 for ~ 4400 μm and ~ 440 μm , respectively. Accordingly, the length of the MFC fibers is far below the critical value. This is in harmony with the tensile yield results which did not differ for the TPS_MFC_10 as a function of the MFC type (cf. Table III). It can be concluded that a similar aspect ratio of microfibrils results in similar tensile properties in TPS/cellulosic fiber microcomposites.

Morphology. Figures 3 reveals SEM images of the failure surface of the prepared samples. Figure 3(a) shows that there are no remaining granular starch particles in the TPS. So, gelatinization of the starch was successful. In Figure 3(b) and (c) the cellulose microfibrils can clearly identified (indicated by circles). Comparing Figure 3(b,c), one can recognize the difference between the sizes of two types of MFC used. The SEM pictures suggest a rather good adhesion between the TPS matrix and the cellulose fibers. The SEM pictures in Figure 3(b) and c also refer to a good dispersion of MFC in the TPS matrix, which is in good agreement with the tensile test results. It can be seen that there are no large MFC agglomerates in the TPS/MFC according to the SEM images. This was further confirmed in the OM images of the samples showing that a homogenous distribution of MFC was achieved by the continuous twin-screw extrusion processing (cf. Figure 4). Comparing Figure 4(c,d) the difference between the cross sections of the B 600 and UFC-100 MFCs becomes obvious. A close look at Figure 4(a,d) substantiates the previous assumption that the inherent mean flaw size of TPS is closely matched with that of the UFC-100 particles.

Dynamic-Mechanical Behavior. The thermo-mechanical properties of the prepared TPS-based biocomposites were investigated by DMA. The diagram in Figure 5 presents the course of the loss factor ($\tan \delta$) and the relative storage modulus as a function of temperature. The relative storage modulus is defined as the ratio between the actual storage modulus (E') and the modulus of the material in its glassy state at $T = -100^\circ\text{C}$ (E'_g). This kind of visualization of the stiffness change as a function of temperature (i.e., E'/E'_g vs. T) is often followed in the literature when analyzing the properties of TPS-based materials.^{14,31} A two-step modulus drop, parallel to the appearance of two $\tan \delta$ peaks, were observed in the relative modulus vs. temperature traces. This is in accordance with the literature.^{14,31,37} Angles *et al.*³⁷ reported that that the glycerol plasticized TPS represents a complex heterogeneous system that contains glycerol-rich domains dispersed in a continuous starch-rich phase. Accordingly, these two phases exhibit their own glass transitions. This has been confirmed by other studies, as well.^{17,38,39} The peak at the lower temperature is attributed to the glass transition temperature of the glycerol-rich domains ($T_{g\beta}$), whereas the peak at higher temperature is connected to the glass transition of the starch-rich phase ($T_{g\alpha}$). As it can be noted, the introduction of 10 wt % MFC into the TPS (regardless of its type) resulted in a shift of $T_{g\alpha}$. The position of $T_{g\beta}$ relaxation does not change with increasing MFC content compared to neat TPS. On the other hand, its intensity was markedly reduced with increasing B 600 MFC. There is only a marginal difference between the DMA traces of TPS_B600 and TPS_UFC with the same amount of MFC (i.e., 10 wt %). This finding is in line with tensile test results. A reduction in the loss factor peaks is always a hint for

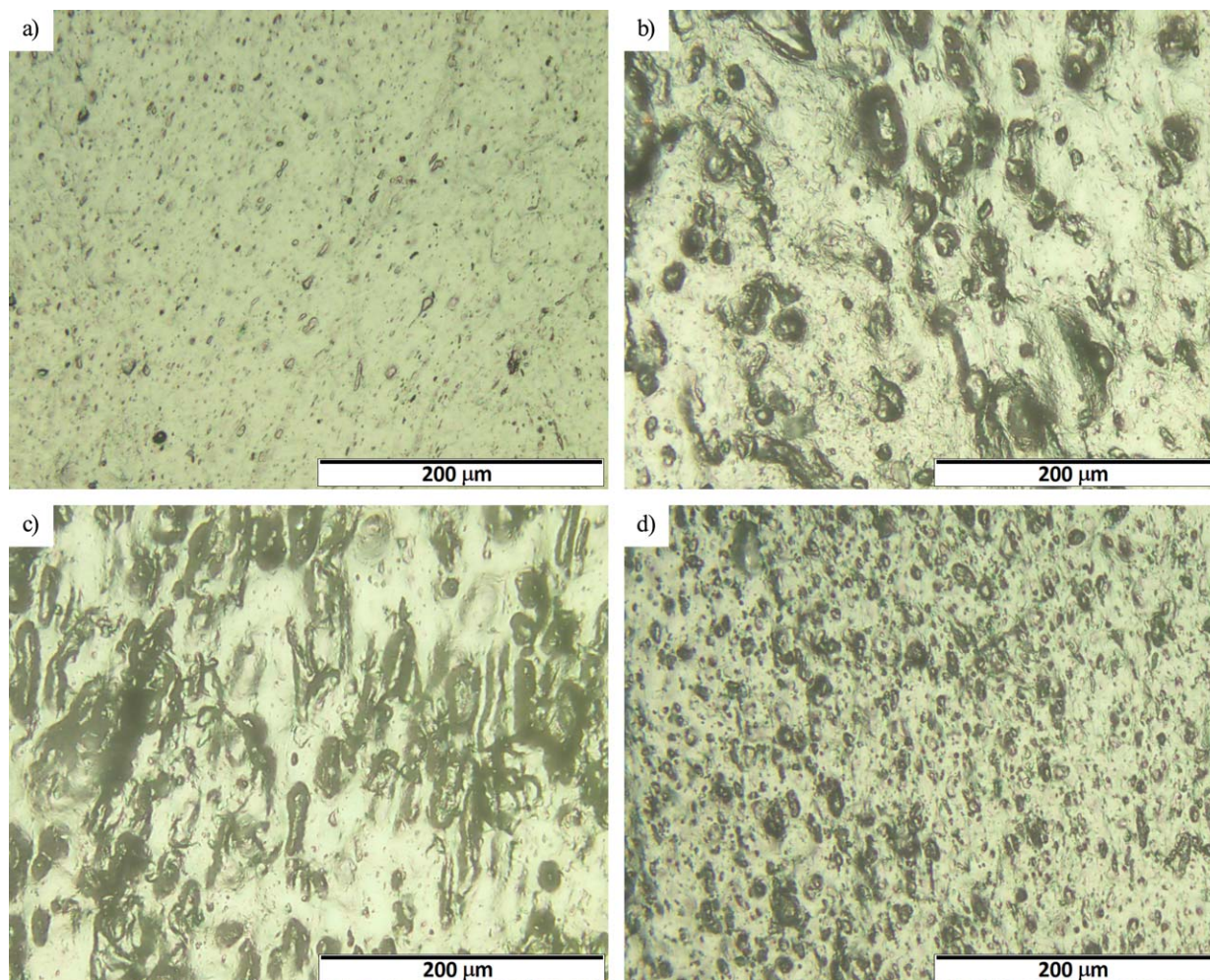


Figure 4. OM images taken from the polished surfaces of TPS (a) and TPS/MFC composites (b,c,d). Designations: (a) TPS, (b) TPS_B600_10, (c) TPS_B600_20, (d) TPS_UFC_10. [Color figure can be viewed in the online issue, which is available at wileyonlinelibrary.com.]

the reinforcing action of the filler. By contrast, T_{gz} shifts toward higher temperature, its peaks is reduced and the related drop in the modulus becomes less with increasing MFC content. This

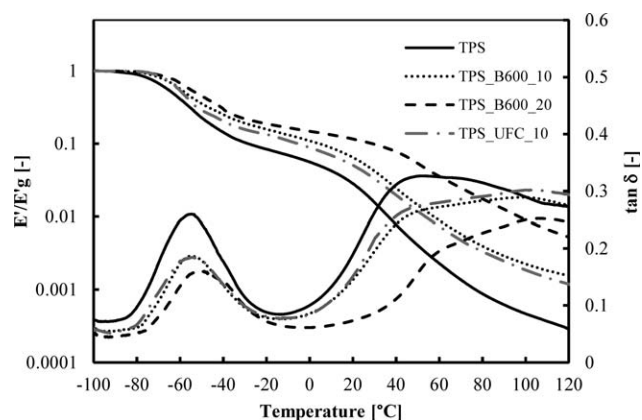


Figure 5. Course of the relative storage modulus (E'/E'_g in semi logarithmic representation) and mechanical loss factor ($\tan \delta$) as a function of temperature for the TPS and its biocomposites with 10 and 20 wt % MFC.

suggests a prominent reinforcement, especially in the starch-based phase, by the MFC incorporated. One can thus conclude that MFC particles are not homogeneously distributed in the two different phases of TPS. The MFC particles strengthen mainly the starch-based phase thereby improving the heat stability of the TPS composite. This finding is in good agreement with the tensile test results, viz. increasing amount of MFC results in an enhanced modulus at room temperature (cf. Table III).

TGA Behavior. TGA was performed to examine how the incorporation of MFC influences the decomposition behavior of the TPS/MFC microcomposites. Figure 6 shows the TGA trace [Figure 6(a)] and its derivative [DTG, Figure 6(b)] for the MFC types used. The weight loss in the TGA and related peak in the DTG traces up to $\sim 100^\circ\text{C}$ represents the evaporation of water adsorbed by the cellulose particles. It can be clearly seen that UFC-100 particles start to decompose $\sim 15^\circ\text{C}$ higher temperature and yield lower ash residue than B 600 MFC.

The TGA traces of TPS and its microcomposites with B 600 MFC are shown in Figure 7. Initial weight loss observed between 50 and 250°C corresponds to the elimination of water

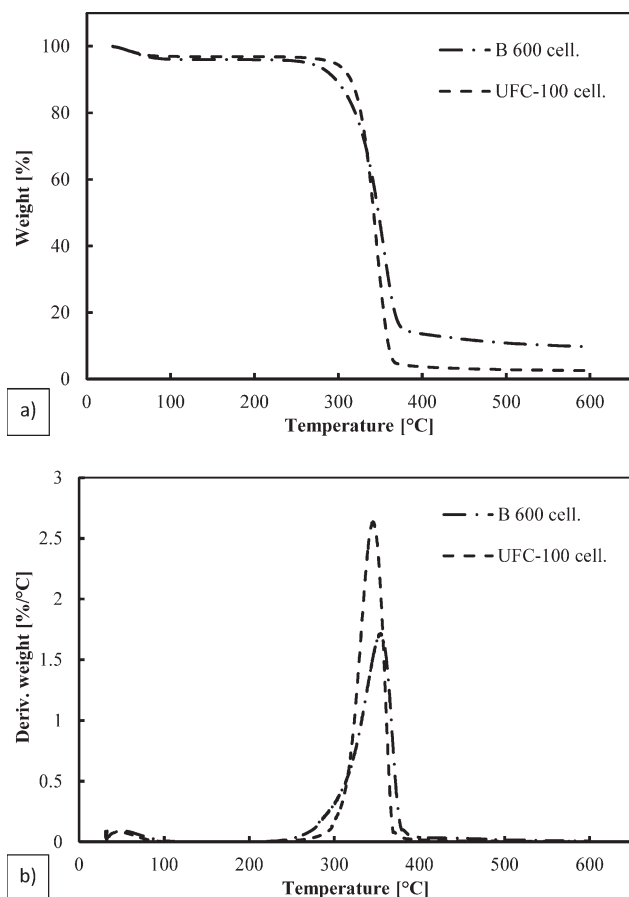


Figure 6. TGA (a) and DTG (b) curves of different types of neat MFCs.

and glycerol, absorbed by starch, along with other low molecular weight compounds.^{25,40} The peak on the DTG curve representing the degradation of the neat TPS is at about 323°C. This is in harmony with literature data.^{15,17,20} Increasing MFC content had little to no effect on the decomposition behavior of TPS. Thus it can be concluded, that the effect of MFC on the thermal stability of TPS is insignificant. DTG curves show that the thermal decomposition of the neat TPS ends at ~355°C, while in case of its MFC a shoulder appears at ~380°C. The latter is associated with the decomposition of the MFC particles [cf. Figure 6(b)].

It has been also observed that the presence of MFC changes the optical properties of the corresponding TPS composites. The initially transparent TPS became more and more opaque with increasing cellulose content. Hietala *et al.*⁹ performed UV/Vis spectroscopic measurements to quantify this effect. They confirmed that the increased light scattering is due to the reinforcing particles. When using TPS or its MFC composites as a packaging materials this aspect should be considered for the target applications.

CONCLUSIONS

On the basis of this study, devoted to improve the mechanical properties of glycerol plasticized thermoplastic starch (TPS) by

incorporation of microfibrillated cellulose (MFC) particles of different characteristics, the following conclusions can be drawn:

- the 4:1 ratio of starch:glycerol with additional water in 1:6 ratio with respect to the overall recipe mass resulted in well gelatinized and plasticized TPS after melt compounding via twin-screw extrusion. The TPS showed two relaxation transitions, both of them with substantial stiffness reductions, which were attributed to the presence of glycerol-rich and starch-rich phases in TPS.
- MFC worked as reinforcement. Its incorporation enhanced the stiffness (Young's modulus), yield strength, however, at cost of the elongation at break. The related changes were amplified with increasing amount of MFC. According to dynamic-mechanical analysis (DMA) MFC acted as reinforcement more efficiently in the starch-rich than in the glycerol-rich phase of TPS
- the MFC types, differing in their average length and diameter values, did not cause any change in the tensile mechanical and DMA properties of the related TPS-based composites when incorporated in the same amount. This was traced to their similar aspect ratios and length values lying far below the critical one.

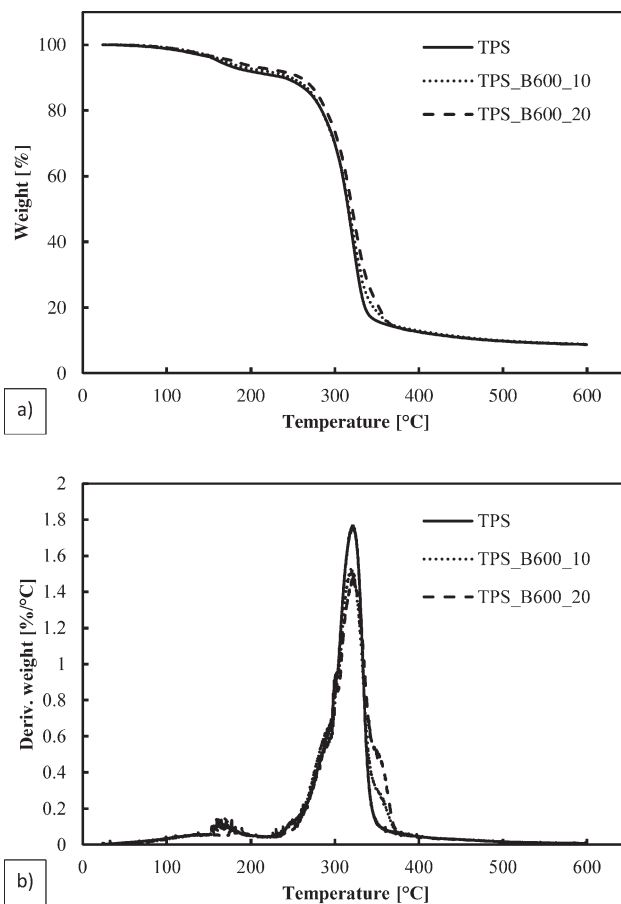


Figure 7. TGA (a) and DTG (b) curves of parent TPS and its microcomposites containing different amounts of B 600 MFC.

- the thermal decomposition behavior of TPS was not influenced by the type and amount of the MFCs incorporated according to TGA tests.

ACKNOWLEDGMENTS

The work reported here was supported by the Hungarian Research Fund (OTKA) through the project K 109409. This research was realized in the frames of TÁMOP 4.2.4. A/1–11–1–2012–0001, National Excellence Program – Elaborating and operating an inland student and researcher personal support system”. The project was subsidized by the European Union and co-financed by the European Social Fund. This work is connected to the scientific program of the “Development of quality-oriented and harmonized R + D + I strategy and functional model at BME” project and supported by the New Széchenyi Plan (Project ID: TÁMOP-4.2.1/B-09/1/KMR-2010-0002). The authors thank Ms. K. Bocz for the TGA measurements.

REFERENCES

1. Shanks, R.; Kong, I. in *Thermoplastic elastomers*; El-Sonbati, A. Z., Ed.; Intech Open: Rijeka, **2012**, Chapter 6, 95.
2. Nafchi, M. A.; Moradpour, M.; Saeidi, M.; Alias, A. K. *Starch* **2013**, *65*, 61.
3. Nasserri, R.; Mohammadi, N. *Carbohydr. Polym.* **2014**, *106*, 432.
4. Tabi, T.; Kovacs, J. G. *Express Polym. Lett.* **2007**, *1*, 804.
5. Xie, F.; Pollet, E.; Halley, P. J.; Avérous, L. *Prog. Polym. Sci.* **2013**, *38*, 1590.
6. Lu, D. R.; Xiao, C. M.; Xu, S. J. *Express Polym. Lett.* **2009**, *3*, 366.
7. Stepto, R. F. T. *Macromol. Symp.* **2000**, *152*, 73.
8. Stepto, R. F. T. *Macromol. Symp.* **2003**, *201*, 203.
9. Hietala, M.; Mathew, A. P.; Oksman, K. *Eur. Polym. J.* **2013**, *49*, 950.
10. Magalhães, N. F.; Andrade, C. T. *J. Brazilian Chem. Soc.* **2010**, *21*, 202.
11. Nasri-Nasrabadi, B.; Behzad, T.; Bagheri, R. *Fibers Polym.* **2014**, *15*, 347.
12. Müller, P.; Kapin, É.; Fekete, E. *Carbohydr. Polym.* **2014**, *113*, 569.
13. Karimi, S.; Dufresne, A.; Md. Tahir, P.; Karimi, A.; Abdulkhani, A. *J. Mater. Sci.* **2014**, *49*, 4513.
14. García, N. L.; Ribba, L.; Dufresne, A.; Aranguren, M.; Goyanes, S. *Carbohydr. Polym.* **2011**, *84*, 203.
15. Schlemmer, D.; Angélica, R. S.; Sales, M. J. A. *Compos. Struct.* **2010**, *92*, 2066.
16. Schmitt, H.; Guidez, A.; Prashantha, K.; Soulestin, J.; Lacrampe, M. F.; Krawczak, P. *Carbohydr. Polym.* **2015**, *115*, 364.
17. Soykeabkaew, N.; Laosat, N.; Ngaokla, A.; Yodsuan, N.; Tunkasiri, T. *Compos. Sci. Technol.* **2012**, *72*, 845.
18. Dai, H.; Chang, P. R.; Yu, J.; Ma, X.; Zhou, P. *Polym. Eng. Sci.* **2010**, *50*, 970.
19. Savadekar, N. R.; Mhaske, S. T. *Carbohydr. Polym.* **2012**, *89*, 146.
20. López, J. P.; Mutjé, P.; Carvalho, A. J. F.; Curvelo, A. A. S.; Gironès, J. *Ind. Crops Products* **2013**, *44*, 300.
21. Ayana, B.; Suin, S.; Khatua, B. B. *Carbohydr. Polym.* **2014**, *110*, 430.
22. Teixeira, E. d. M.; Curvelo, A. A. S.; Corrêa, A. C.; Marconcini, J. M.; Glenn, G. M.; Mattoso, L. H. C. *Ind. Crops Products* **2012**, *37*, 61.
23. Arroyo, O. H.; Huneault, M. A.; Favis, B. D.; Bureau, M. N. *Polym. Compos.* **2010**, *31*, 114.
24. Ren, J.; Fu, H.; Ren, T.; Yuan, W. *Carbohydr. Polym.* **2009**, *77*, 576.
25. Cyras, V. P.; Manfredi, L. B.; Ton-That, M.-T.; Vázquez, A. *Carbohydr. Polym.* **2008**, *73*, 55.
26. Hietala, M.; Rollo, P.; Kekäläinen, K.; Oksman, K. *J. Appl. Polym. Sci.* **2014**, *131*, 39981.
27. Turbak, A. F. *J. Appl. Polym. Sci.: Appl. Polym. Symp* **1983**, *37*, 815.
28. Zhu, C.; Chen, J.; Koziol, K. K.; Gilman, J. W.; Trulove, P. C.; Rahatekar, S. S. *Express Polym. Lett.* **2014**, *8*, 154.
29. Chen, W. J.; Gu, J.; Xu, S. H. *Express Polym. Lett.* **2014**, *8*, 659.
30. Cao, X.; Chen, Y.; Chang, P. R.; Muir, A. D.; Falk, G. *Express Polym. Lett.* **2008**, *2*, 502.
31. González, K.; Retegi, A.; González, A.; Eceiza, A.; Gabilondo, N. *Carbohydr. Polym.* **2015**, *117*, 83.
32. Karger-Kocsis, J. in *Nano- and Micromechanics of Polymer Blends and Composites*; Karger-Kocsis, J.; Fakirov, S., Eds.; Carl Hanser Verlag GmbH & Co. KG: Munich, Germany, **2009**, Chapter 12, 425.
33. Tjong, S. C. *Mater. Sci. Eng. R: Rep.* **2006**, *53*, 73.
34. Karger-Kocsis, J.; Kmetty, Á.; Lendvai, L.; Drakopoulos, S.; Bárány, T. *Materials* **2015**, *8*, 72.
35. Rodríguez-Gonzalez, F. J.; Ramsay, B. A.; Favis, B. D. *Carbohydr. Polym.* **2004**, *58*, 139.
36. Aitomäki, Y.; Oksman, K. *Reactive Funct. Polym.* **2014**, *85*, 151.
37. Anglès, M. N.; Dufresne, A. *Macromolecules* **2000**, *33*, 8344.
38. Teixeira, E. d. M.; Pasquini, D.; Curvelo, A. A. S.; Corradini, E.; Belgacem, M. N.; Dufresne, A. *Carbohydr. Polym.* **2009**, *78*, 422.
39. Forssell, P. M.; Mikkilä, J. M.; Moates, G. K.; Parker, R. *Carbohydr. Polym.* **1997**, *34*, 275.
40. Martins, I. M. G.; Magina, S. P.; Oliveira, L.; Freire, C. S. R.; Silvestre, A. J. D.; Neto, C. P.; Gandini, A. *Compos. Sci. Technol.* **2009**, *69*, 2163.